Cell

IAP Antagonists Induce Autoubiquitination of c-IAPs, NF-κB Activation, and TNFα-Dependent Apoptosis

Eugene Varfolomeev,[1] John W. Blankenship,[1] Sarah M. Wayson,[1] Anna V. Fedorova,[1] Nobuhiko Kayagaki,[2] Parie Garg,[2] Kerry Zobel,[1] Jasmin N. Dynek,[1] Linda O. Elliott,[3] Heidi J.A. Wallweber,[1] John A. Flygare,[3] Wayne J. Fairbrother,[1] Kurt Deshayes,[1] Vishva M. Dixit,[2,*] and Domagoj Vucic[1,*]
[1]Department of Protein Engineering
[2]Department of Physiological Chemistry
[3]Department of Medicinal Chemistry
Genentech, Inc., South San Francisco, CA 94080, USA
*Correspondence: domagoj@gene.com (D.V.), dixit@gene.com (V.M.D.)
DOI 10.1016/j.cell.2007.10.030

SUMMARY

Inhibitor of apoptosis (IAP) proteins are anti-apoptotic regulators that block cell death in response to diverse stimuli. They are expressed at elevated levels in human malignancies and are attractive targets for the development of novel cancer therapeutics. Herein, we demonstrate that small-molecule IAP antagonists bind to select baculovirus IAP repeat (BIR) domains resulting in dramatic induction of autoubiquitination activity and rapid proteasomal degradation of c-IAPs. The IAP antagonists also induce cell death that is dependent on TNF signaling and de novo protein biosynthesis. Additionally, the c-IAP proteins were found to function as regulators of NF-κB signaling. Through their ubiquitin E3 ligase activities c-IAP1 and c-IAP2 promote proteasomal degradation of NIK, the central ser/thr kinase in the noncanonical NF-κB pathway.

INTRODUCTION

Apoptosis or programmed cell death is a cell suicide mechanism with a major role in development and homeostasis in vertebrates and invertebrates (Steller, 1995). Inhibition of apoptosis can lead to the absence of physiological cell death and contribute to development and progression of various malignancies (Thompson, 1995). There are two well-characterized apoptotic pathways; one initiated through the engagement of cell surface death receptors by their specific ligands (Ashkenazi and Dixit, 1999) and the other triggered by changes in internal cellular integrity (Budihardjo et al., 1999; Kaufmann and Vaux, 2003). Both pathways converge, resulting in activation of caspases—*c*ysteine-dependent *asp*artyl-specific proteases—that represent the effector arm of the apoptotic process (Salvesen and Abrams, 2004). Inhibition of apoptosis enhances the survival of cancer cells and facilitates their escape from immune surveillance and cytotoxic therapies (Reed, 2003). Among the principal molecules contributing to this phenomenon are the inhibitor of apoptosis (IAP) proteins (Hunter et al., 2007).

IAP proteins interact with multiple cellular partners and inhibit apoptosis induced by a variety of stimuli (Salvesen and Duckett, 2002). This places IAPs in a central position as inhibitors of death signals that proceed through a number of different pathways (Miller, 1999). The IAP proteins contain one to three zinc-binding baculovirus IAP repeat (BIR) domains that are required for anti-apoptotic activity (Liston et al., 2003; Salvesen and Duckett, 2002). Most of them also possess carboxy-terminal RING domains that function as ubiquitin ligases (Salvesen and Duckett, 2002; Vaux and Silke, 2005). Some IAP proteins, like c-IAP1 and c-IAP2, possess a caspase-associated recruitment domain (CARD) as well (Hofmann et al., 1997). c-IAP1 and c-IAP2 were originally identified through their ability to interact directly with tumor necrosis factor associated factors (TRAFs), namely TRAF2 (Rothe et al., 1995, 1994). Through TRAF2 interactions, c-IAP1 and c-IAP2 are recruited to TNF receptor 1- and 2-associated complexes where they regulate receptor-mediated apoptosis (Shu et al., 1996; Wang et al., 1998). c-IAPs and TRAF2 associate through their BIR and TRAF-N domains (Rothe et al., 1995) respectively. Recent studies indicate that the first two alpha-helices in the BIR1 domain of c-IAP1 and c-IAP2 are critical for that interaction (Samuel et al., 2006; Varfolomeev et al., 2006). c-IAP1 and c-IAP2 are also RING domain-containing ubiquitin ligases capable of promoting ubiquitination and proteasomal degradation of themselves and several of their binding partners (Li et al., 2002; Vaux and Silke, 2005; Yang et al., 2000).

The anti-apoptotic activity of IAP proteins can be negated by the mitochondrial protein SMAC (second mitochondrial activator of caspases)/DIABLO (direct IAP

binding protein with low pI), which is liberated into the cytoplasm in response to pro-apoptotic stimuli (Du et al., 2000; Verhagen et al., 2000). The pro-apoptotic function of SMAC/DIABLO is dependent on a conserved four-residue IAP-interaction motif (Ala–Val–Pro–Ile) found at the amino-terminus of the mature, post-translationally processed protein (Du et al., 2000; Verhagen et al., 2000). This IAP-interaction motif binds to a surface groove on the BIR domains of the IAP proteins (Liu et al., 2000; Wu et al., 2000). A number of IAP antagonists that mimic the interactions of the SMAC amino-terminal peptide with IAP proteins have been reported recently, and been shown to possess pro-apoptotic activity both in vitro and in vivo (Li et al., 2004; Oost et al., 2004; Sharma et al., 2006; Sun et al., 2004; Zobel et al., 2006). These IAP antagonists effectively block the interaction between IAP proteins and activated caspase-9 (Li et al., 2004; Sharma et al., 2006; Zobel et al., 2006), resulting in unimpeded caspase activation, although the mechanism by which these compounds initiate the apoptotic cascade is not entirely clear (Oost et al., 2004).

Here we describe development of a novel class of small-molecule IAP antagonists that bind to the BIR domains of IAP proteins leading to rapid ubiquitination and proteasomal degradation of c-IAPs. We discover that c-IAP proteins are important regulators of NF-κB signaling and ubiquitin ligases for the critical kinase in the noncanonical NF-κB pathway, NIK. Finally, we establish that IAP antagonist-induced cell death is dependent on TNF signaling. These functional and mechanistic data provide a molecular platform for the rational development of a novel class of cancer therapeutics.

RESULTS

Biophysical Analysis of IAP Protein-IAP Antagonist Interactions

To elucidate the mechanism of IAP antagonism, structure-based design was used to generate novel, monovalent (MV1) and bivalent (BV6) compounds that target IAP proteins (Figure 1A and Figure S1 in the Supplemental Data available with this article online). Both MV1 and BV6, but not their enantiomers, MVE1 and BVE6, antagonize IAP protein-protein interactions as exemplified by disruption of XIAP – caspase-9 association (Figure S2). Binding affinities of the monovalent and bivalent IAP antagonists were determined by surface plasmon resonance (SPR), employing biotinylated versions of MV1 and BV6 as analytes (MV1-B and BV6-B, respectively) and recombinant IAP proteins (XIAP and c-IAP1) containing BIR2, BIR3, or both BIR2 and BIR3 domains as ligands (Table 1). As reported previously for SMAC-derived peptides (Liu et al., 2000), the monovalent SMAC-based antagonist displayed tighter binding to the BIR3 domains relative to the BIR2 domains. The bivalent antagonist displayed similar affinities for the BIR2-BIR3 domain constructs, although the interactions could be only fit using a two-site binding model. The stronger, first-site affinities were essentially equal to the binding affinities of the BIR3 constructs for MV1-B, and the second-site affinities were greater than the measured affinities of the BIR2 constructs for MV1-B (Table 1). These increased affinities may reflect improved binding to the BIR2 domains, corresponding to a probable increase in the effective concentration of the antagonist at the BIR2 domains due to the bivalent linkage (XIAP, see below), or the dimerization of two IAP proteins through the bivalent linkage of two BIR3 domains (c-IAP1, see below). Fluorescence polarization competition assays were also used to study binding of MV1, BV6, and their enantiomers, MVE1 and BVE6, to the BIR2 and BIR3 domains of XIAP, c-IAP1, and c-IAP2 in solution. Observed binding affinities for MV1 and BV6 were similar to those determined by SPR analysis, while the enantiomeric compounds did not display significant binding to any of the BIR domains (Table S2).

Analytical ultracentrifugation was used to further investigate the binding mode of MV1 and BV6 to the c-IAP1 and XIAP BIR2-BIR3 domains (Tables 1 and S3). Both c-IAP1 and XIAP BIR2-BIR3 domains were monomeric in the absence of antagonists and in the presence of up to a 30-fold excess of MV1, as assessed by sedimentation velocity and equilibrium experiments. XIAP BIR2-BIR3 also remained monomeric with the addition of BV6, even at high concentrations, suggesting that BV6 binds intramolecularly to both the BIR2 and BIR3 domains of XIAP. In contrast, BV6 induced dimerization of c-IAP1 BIR2-BIR3, plateauing at 0.6 equivalents of BV6 to c-IAP1, suggesting that one molecule of BV6 binds the BIR3 domains of two c-IAP1 molecules, and that the second affinity observed in SPR analysis is the result of a reduced binding affinity (by one order of magnitude) to a second c-IAP1 BIR3 domain rather than an increased affinity (by four orders of magnitude) to the c-IAP1 BIR2 domain.

IAP Antagonists Trigger Rapid Proteasomal Degradation of c-IAP1 and c-IAP2

Next, the effects of the monovalent and bivalent IAP antagonists on the stability of IAP proteins were examined. Treatment of MDA-MB-231 breast carcinoma cells with BV6 lead to a precipitous loss of c-IAP1 and 2 proteins (Figure 1B). The levels of XIAP, TRAF2, TRAF5, caspase-3, and caspase-8 proteins were unperturbed except at the 12h time point, coincident with the observed activation of caspases 8 and 3 and induction of apoptosis (Figure 1B and data not shown). When MDA-MB-231 cells were treated with MV1 or BV6 for much shorter time periods, the c-IAP1 and 2 protein levels were found to decrease significantly by as early as two minutes following exposure (Figure 1C). This striking and prompt loss of c-IAP proteins following treatment with MV1 or BV6 was not due to sequestration of the proteins to the insoluble fraction of the cellular lysates because direct lysis of cells in SDS-containing buffer confirmed the rapid loss of these proteins following treatment (Figure S3). The decrease in c-IAP1 and 2 protein levels was dependent on the concentrations

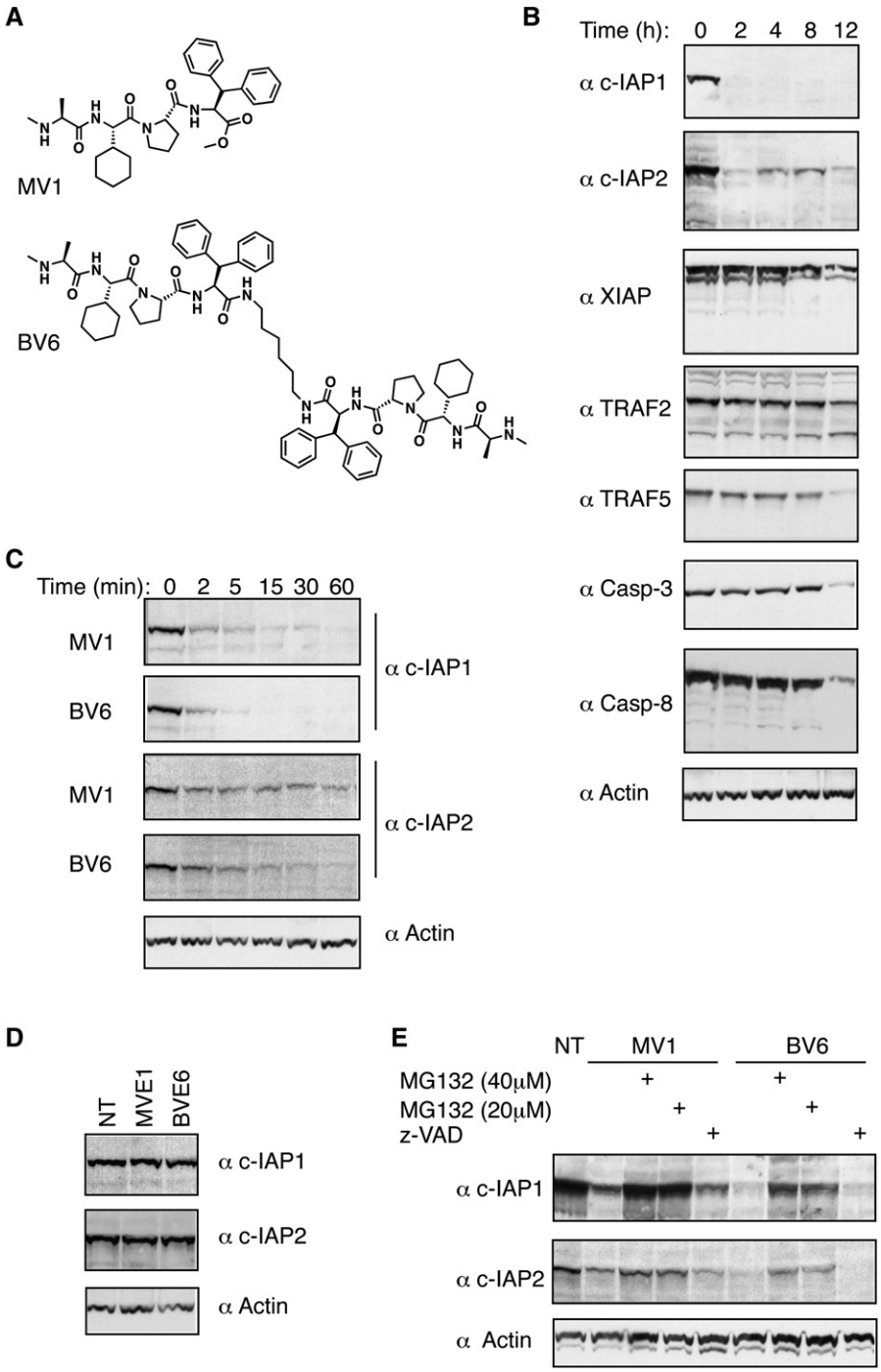

Figure 1. Monovalent and Bivalent IAP Antagonists Trigger Rapid Proteasomal Degradation of c-IAP1 and c-IAP2

(A) The structure of monovalent (MV1) and bivalent (BV6) IAP antagonists.

(B) Treatment with IAP antagonists leads to degradation of c-IAP1 and 2. MDA-MB-231 cells were treated with BV6 (5 μM) for the indicated time periods and cell lysates were probed with the indicated antibodies.

(C) Monovalent and bivalent IAP antagonists cause rapid loss of c-IAP1 and c-IAP2. MDA-MB-231 cells were treated with MV1 or BV6 (5 μM) for the indicated time periods and cell lysates were examined by Western blotting using antibodies against c-IAP1 and c-IAP2.

(D) Degradation of c-IAP1 and c-IAP2 induced by IAP antagonists is specific. MDA-MB-231 cells were treated with MVE1 and BVE6 (all at 5 μM) for 1 hr and cellular lysates were examined by Western blotting using antibodies against c-IAP1 and c-IAP2.

(E) IAP antagonist-induced degradation of c-IAP1 and c-IAP2 is dependent on proteasomal machinery but not on caspase activation. MDA-MB-231 cells were treated with MV1 or BV6 (5 μM) for 1 hr in the absence or presence of proteasome inhibitor (20 μM MG132) or caspase inhibitor (z-VAD; 25 μM) and cell lysates were examined by Western blotting using antibodies against c-IAP1 and c-IAP2.

Table 1. Biophysical Effects of IAP Protein-IAP Antagonist Interactions

Protein	Antagonist	K_D site I (nM)[a]	K_D site II (μM)[a]	AUC[b]
c-IAP1				
BIR2	MV1-B	—	220 ± 240	
BIR3	MV1-B	5.8 ± 2.1	—	
BIR2-BIR3	—			monomer
BIR2-BIR3	MV1-B	1.00 ± 0.26	—	monomer
BIR2-BIR3	BV6-B	0.46 ± 0.31	0.029 ± 0.011	mono ↔ dimer
XIAP				
BIR2	MV1-B	—	28 ± 15	
BIR3	MV1-B	16.0 ± 8.9	—	
BIR2-BIR3	—			monomer
BIR2-BIR3	MV1-B	1.00 ± 0.55	—	monomer
BIR2-BIR3	BV6-B	1.30 ± 0.25	4.3 ± 2.6	monomer

[a]Apparent dissociation constants for the BIR2 and BIR3 domains of c-IAP1 and XIAP as determined by SPR analysis against biotinylated versions of antagonists MV1 and BV6. For full rate information, see Table S1.
[b]Oligomerization state of the BIR2-BIR3 domains of c-IAP1 and XIAP in the presence and absence of nonbiotinylated IAP antagonists, as determined through sedimentation equilibrium analysis. For more information, see Table S3.

of MV1 or BV6, with higher concentrations being required for comparable decreases in c-IAP2 levels relative to c-IAP1 (Figure S4). Notably, the ability of the antagonists to induce dimerization was not necessary to induce the loss of c-IAP1 and 2. In contrast, the enantiomers of MV1 and BV6, MVE1 and BVE6 respectively, did not affect the levels of c-IAP1 or 2, even at high concentrations (Figure 1D).

Since the IAP antagonists MV1 and BV6 induce cell death in cancer cells (discussed below and shown in Figure 3), the observed loss of c-IAP1 and 2 proteins may be a consequence of the activation of apoptosis (although this seems unlikely given the rapid kinetics). In addition, however, c-IAP1 and 2 are ubiquitin E3 ligases that are capable of mediating auto-ubiquitination and ubiquitination of several of their binding partners (Li et al., 2002; Vaux and Silke, 2005; Yang and Du, 2004), suggesting that their loss following treatment with the IAP antagonists may be the result of proteasome-mediated degradation. To address these possible mechanisms of IAP antagonist-induced loss of c-IAP1 and 2, MDA-MB-231 cells were treated with MV1 or BV6 in the absence or presence of either the pan-caspase inhibitor z-VAD or the proteasome inhibitor MG132. The presence of MG132 efficiently blocked the IAP antagonist-dependent decreases in c-IAP1 and 2 protein levels, while administration of z-VAD had no effect (Figure 1E). This proteasome-mediated degradative effect of IAP antagonists was observed in all cell lines tested suggesting that it might be a general phenomenon (Figure S5). Thus, IAP antagonists stimulate proteasomal degradation of c-IAP1 and 2 that is independent of caspase activation.

To determine which portions of c-IAP1 and 2 are required for IAP antagonist-induced degradation, an overexpression system was established in 293T cells and Flag-tagged c-IAP1 and 2 proteins were demonstrated to be similarly degraded in a proteasome-dependent fashion upon treatment with MV1 or BV6 (Figures 2A, 2B, and S6). In agreement with earlier experiments, the IAP antagonists did not affect protein levels of Flag-tagged XIAP and ML-IAP or of endogenous TRAF2 and TRAF5 (Figure 2A). MV1 and BV6 bind to the BIR2 domain of c-IAP1 with low affinities and to the BIR3 domain with high affinities, therefore key contact residues were mutated to alanine in both domains of c-IAP1 (Liu et al., 2000) and the effect of these mutations on the stability of c-IAP1 protein following treatment with the IAP antagonists investigated. In contrast to wild-type c-IAP1, the mutant c-IAP1 protein levels were unchanged (Figure 2C). In order to test the hypothesis that auto-ubiquitination of c-IAP1 might be required for IAP antagonist-induced degradation, one of the zinc-coordinating residues in the ubiquitin E3 ligase RING domain of c-IAP1 (histidine 588) was mutated to alanine. As observed for the BIR2/3-domain mutant, treatment with MV1 or BV6 had no effect on the protein levels of the c-IAP1 RING-domain mutant (Figure 2C). Additionally, in agreement with published observations showing simultaneous interaction of c-IAP1 with SMAC and TRAF2 (Samuel et al., 2006), IAP antagonists did not affect c-IAP1 binding to TRAF2 (Figure S7). Having established that auto-ubiquitination is required for the degradative effect of the IAP antagonists on c-IAP1, we endeavored to reconstitute the ubiquitination process with purified components in vitro. To this end recombinant full-length c-IAP1 protein was incubated with E1 and E2 (UbcH5a) enzymes in an ubiquitination assay in the absence or presence of BV6 or MV1 (Figure 2D). After as little as three minutes both BV6 and MV1 triggered significant auto-ubiquitination of c-IAP1 that was more pronounced

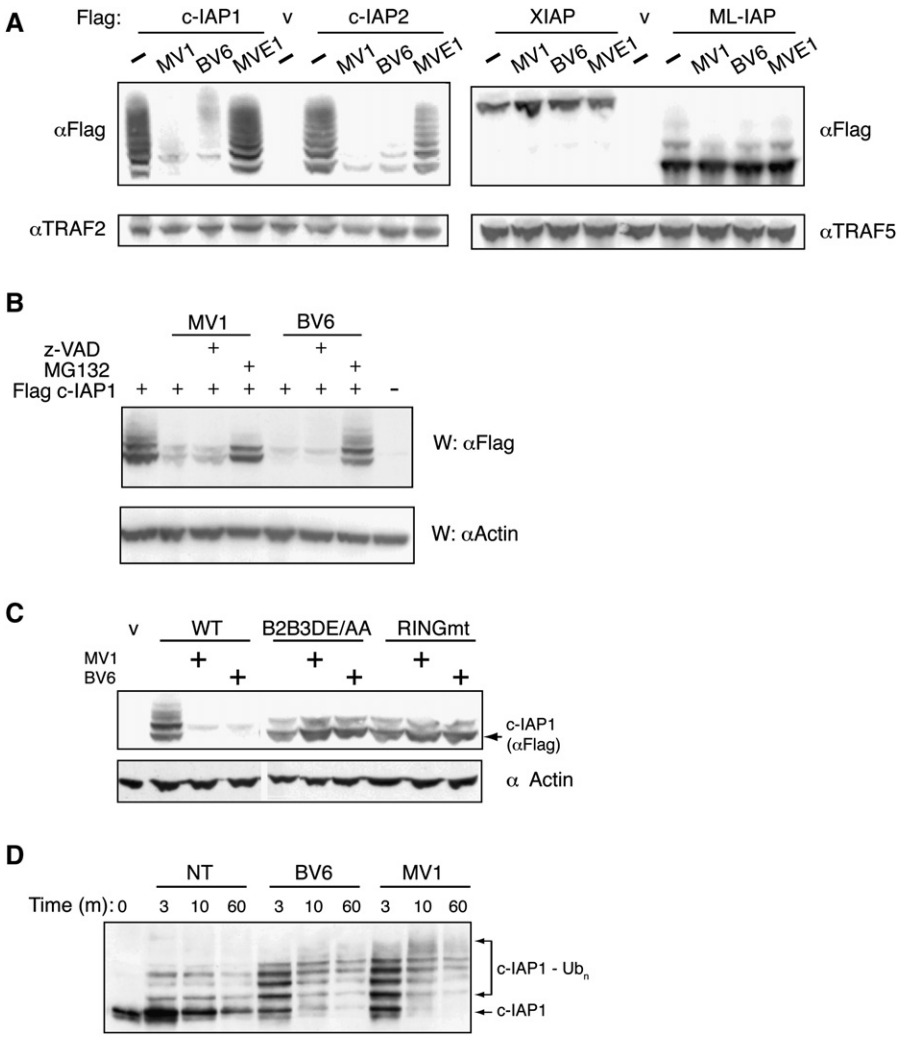

Figure 2. IAP Antagonist-Mediated Degradation of c-IAP1 Requires BIR and RING Domains

(A) HEK293T cells were transiently transfected with indicated Flag-tagged IAP constructs and 24 hr later treated with 5 μM of MV1, BV6, MVE1, or PBS for 1 hr. Following treatment, cells were lysed in Nonidet P-40 lysis buffer and expression levels of Flag-tagged IAP proteins and endogenous TRAF2 and TRAF5 were determined by immunoblotting with the indicated antibodies.

(B) 293T cells were transiently transfected with Flag-tagged c-IAP1 construct and 24 hr later pre-treated with or without 20 μM MG132 or 25 μM zVAD for 20 min followed by treatment with 5 μM of MV1 or BV6 for 1 hr. After treatment, cells were lysed in Nonidet P-40 lysis buffer and expression levels of c-IAP1 protein were determined by immunoblotting with anti-Flag antibody.

(C) 293T cells were transfected with vector (v), or cDNA constructs encoding Flag-tagged wild-type c-IAP1, BIR2 and BIR3 mutant (D234A/E239A/D320A/E325A; B2B3DE/AA), or RING domain point mutant (H588A; RINGmt). 24 hr after transfection, cells were treated with MV1 or BV6 (5 μM) for 1 hr. Expression of c-IAP1 proteins was analyzed using anti-Flag antibodies.

(D) IAP antagonists stimulate auto-ubiquitination of c-IAP1. Recombinant c-IAP1 (0.2 μM) purified from bacteria was incubated at 21°C in the absence or presence of MV1 or BV6 (1 μM each) in the ubiquitination reaction for the indicated time periods and detected with anti-c-IAP1 antibodies.

than in the absence of the IAP antagonists (Figure 2D). This is consistent with the notion that auto-ubiquitination of c-IAP1 is induced by the IAP antagonists independent of additional cellular factors (Figure 2D). Collectively, these results demonstrate that both monovalent and bivalent IAP antagonists trigger auto-ubiquitination and subsequent rapid proteasomal degradation of c-IAP1 and 2.

Monovalent and Bivalent IAP Antagonists Induce TNFα-Dependent Cell Death

Antagonism of IAP proteins has been shown to provoke apoptosis in cancer cell lines (Li et al., 2004; Oost et al., 2004; Sun et al., 2004; Zobel et al., 2006). To evaluate whether monovalent and bivalent IAP antagonists can induce cell death, MDA-MB-231 and EVSA-T breast cancer and A2058 melanoma cell lines were treated with MV1 or

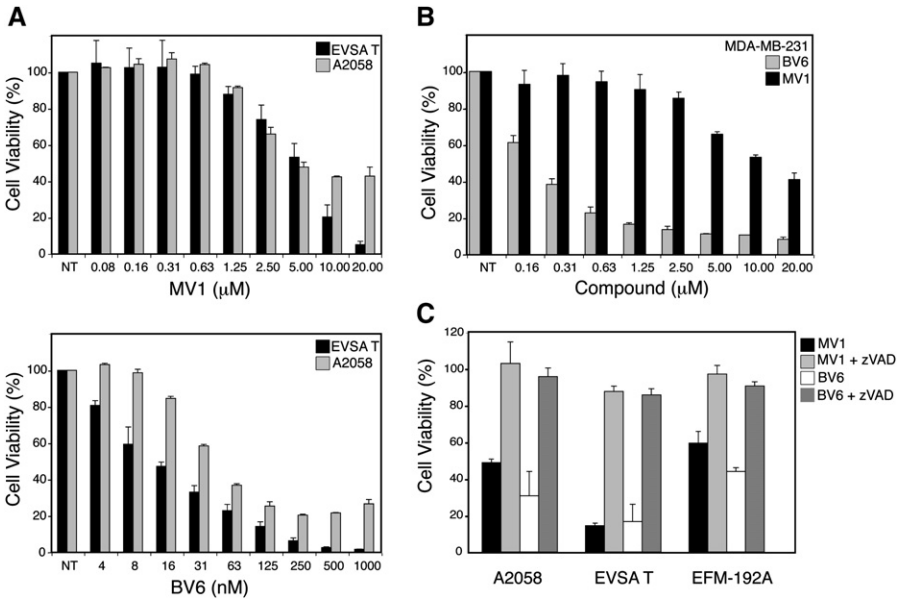

Figure 3. IAP Antagonists Induce Cell Death

(A and B) EVSAT, A2058 (A) and MDAMB-231 (B) cells were treated with increasing amounts of MV1 and BV6 for 24 hr. Cell viability was determined as described in Experimental Procedures.

(C) IAP antagonists trigger caspase-dependent cell death. Cells were treated with MV1 or BV6 (4 μM each) alone or in the presence of z-VAD (25 μM) for 24 hr. Results indicate mean with standard deviation from at least three independent experiments.

BV6 (Figures 3A and 3B). Both IAP antagonists exhibited single-agent cell killing activity with approximate IC_{50} values of 5 μM and 14 nM, respectively, in the highly sensitive EVSA-T cell line (Figure 3A). The enantiomers MVE1 and BVE6 did not induce any appreciable cell death in all cell lines tested (Figure S8). Cotreatment of several cancer cell lines with the caspase inhibitor z-VAD inhibited IAP antagonist-induced apoptosis (Figure 3C), demonstrating that MV1 and BV6 stimulated cell killing is caspase dependent.

Previous studies have shown that the cytotoxic activity of IAP antagonists can be enhanced by administration of TRAIL/Apo2L or TNFα (Li et al., 2004). In concurrence with these reports we observed decreased viability upon treatment of cells with recombinant TNFα, or by expression of TNFα cDNA in the presence of BV6 or MV1 (Figures 4A and S9). Additionally, through TRAF2 interactions c-IAP1 and 2 associate with the TNFR1 signaling complexes and regulate receptor-mediated apoptosis (Micheau and Tschopp, 2003; Rothe et al., 1995; Shu et al., 1996; Wang et al., 1998). Therefore, to examine if cell death induced by IAP antagonists depends upon signaling through TNF family death receptors, cells were treated with BV6 in the presence of TNFR1-Fc, DR5-Fc, or Fas-Fc fusion proteins that would neutralize the respective ligands of the receptor chimeras. Only TNFR1-Fc fusion protein afforded protection from BV6-induced cell death (Figure 4B). The functional inhibitory activities of the Fc-fusion proteins used in these studies were confirmed by cotreatment with their cognate ligands (Figure S10). In addition, small interfering RNA oligonucleotides targeting TNFR1 or TNFα-blocking antibodies provided similar protective effects (Figure 4C and data not shown). The importance of TNF signaling for IAP-mediated cell death was also examined in a clonogenic assay. Inhibition of TNF signaling offered protection to cells from IAP antagonist-stimulated apoptosis and resulted in long-term survival (Figures 4D and S11). Similarly, suppression of TNF signaling prevented cell death induced by the overexpression of the natural IAP antagonist SMAC (Figure S12). To investigate the functional importance of apical caspases in IAP antagonist-induced cell death, we used small interfering RNA oligonucleotides to downregulate the expression of caspase-8 or caspase-9 (Figure 4C). Caspase-8 targeting siRNAs provided significant protection from apoptosis induced by treatment with IAP antagonist BV6 alone or in combination with TNFα (Figure 4C). On the other hand, downregulation of caspase-9 did not have any significant effect on this cell death stimulus (Figure 4C) suggesting that caspase-8 is a critical apoptotic protease in IAP antagonist-induced cell death. Thus, the pro-apoptotic activity of IAP antagonists is mediated by caspase-8 and dependent upon TNF signaling.

IAP Antagonists Activate the Canonical and Noncanonical NF-κB Pathways

These findings prompted us to investigate the signaling pathways that are regulated by TNFR1, including the canonical and noncanonical NF-κB pathways, especially given that the c-IAP1 and 2-interacting adaptor protein, TRAF2, plays a major role in both pathways (Chen and Goeddel, 2002; Grech et al., 2004). First, the effects of

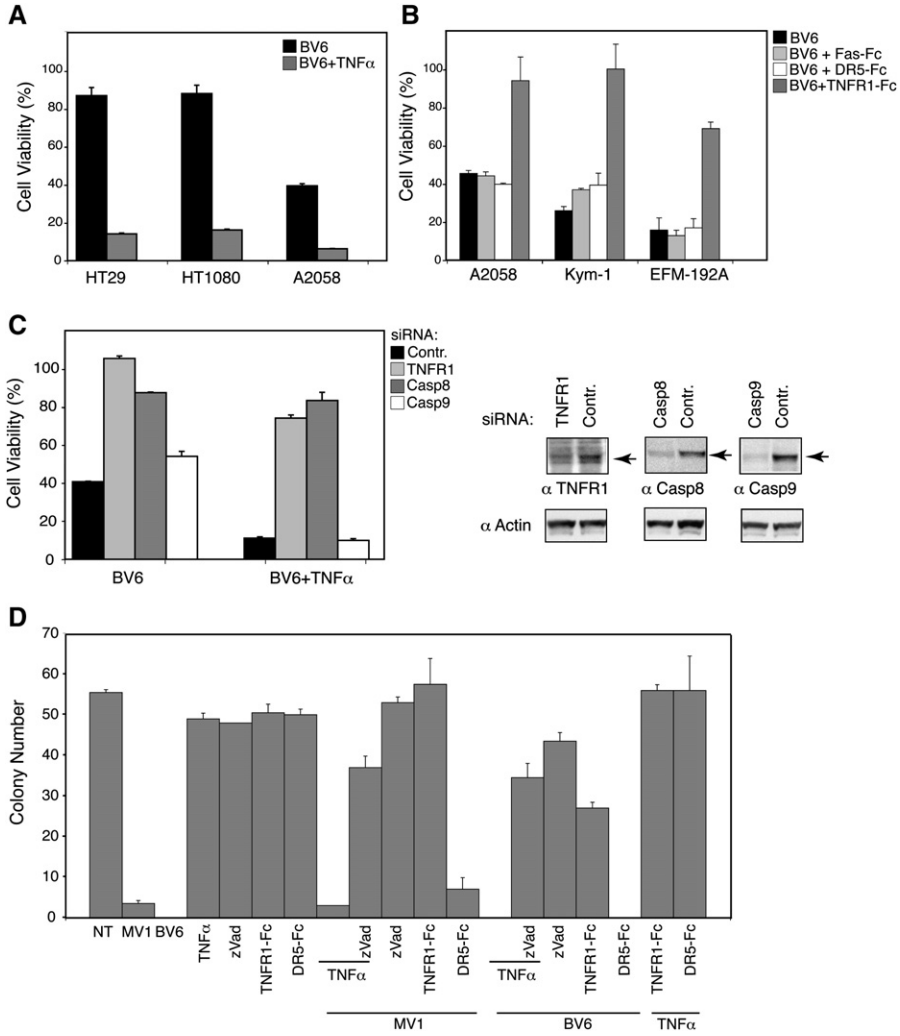

Figure 4. Cell Death Induction by IAP Antagonists Is TNF Dependent

(A) IAP antagonists synergize with TNFα. Indicated cell lines were treated with BV6 (0.6 μM) in the absence or presence of TNFα (1 ng/ml). Cell viability was determined as described in Experimental Procedures.

(B) Indicated cell lines were treated with MV1 (1 μM) or BV6 (100 nM) alone or in the presence of the indicated recombinant fusion proteins (2 μg/ml) for 24 hr. Cell viability was determined as described in Experimental Procedures.

(C) IAP antagonist triggers TNFR1- and caspase-8-dependent cell death. A2058 cells were transfected with control scramble (Contr), TNFR1, caspase-8, or caspase-9 small interfering RNA duplexes. 48 hr later, cells were treated with BV6 (400 nM) alone or with BV6 (200 nM) in the presence of TNFα (1 ng/ml). Right portion of the panel; Expression of TNFR1, caspase-8 and caspase-9 in A2058 cells transfected with gene-specific or scrambled (control) small interfering duplexes was examined by Western blot analysis using indicated antibodies.

(D) Blockade of TNF signaling affords long-term clonogenic survival to IAP antagonist-treated cells. EFM-192A cells were treated with MV1 (0.5 μM) or BV6 (0.25 μM) in the absence or presence of TNFα (20 ng/ml), zVAD (20 μM), TNFα plus zVAD, TNFR1-Fc (5 μg/ml), or DR5-Fc (5 μg/ml), plated, and the average number of colonies was determined 10 days later.

Results indicate mean with standard deviations from three independent experiments.

administration of MV1 or BV6 on production of TNFα, a well-established target of NF-κB signaling, were investigated. The IAP antagonists, but not their enantiomers, induced a 15- to 30-fold increase in *TNFα* mRNA levels compared to untreated cells (Figure 5A). The IAP antagonists also stimulated the mRNA expression of other NF-κB-regulated genes, *MCP-1* and *IL-8* (Figures 5A and S13). In agreement with its ability to induce TNF-dependent cell death, overexpression of SMAC also led to increased level of TNFα mRNA expression (data not shown). Phosphorylation of IκB followed by its proteasomal degradation is a critical event in the canonical NF-κB signaling cascade allowing nuclear translocation of p50:RelA or other NF-κB heterodimer complexes (Hayden and Ghosh, 2004; Scheidereit, 2006). Treatment with BV6 induced phosphorylation and subsequent proteasomal degradation of IκB in several cell lines with kinetics comparable to treatment with TNFα. (Figures 5B and

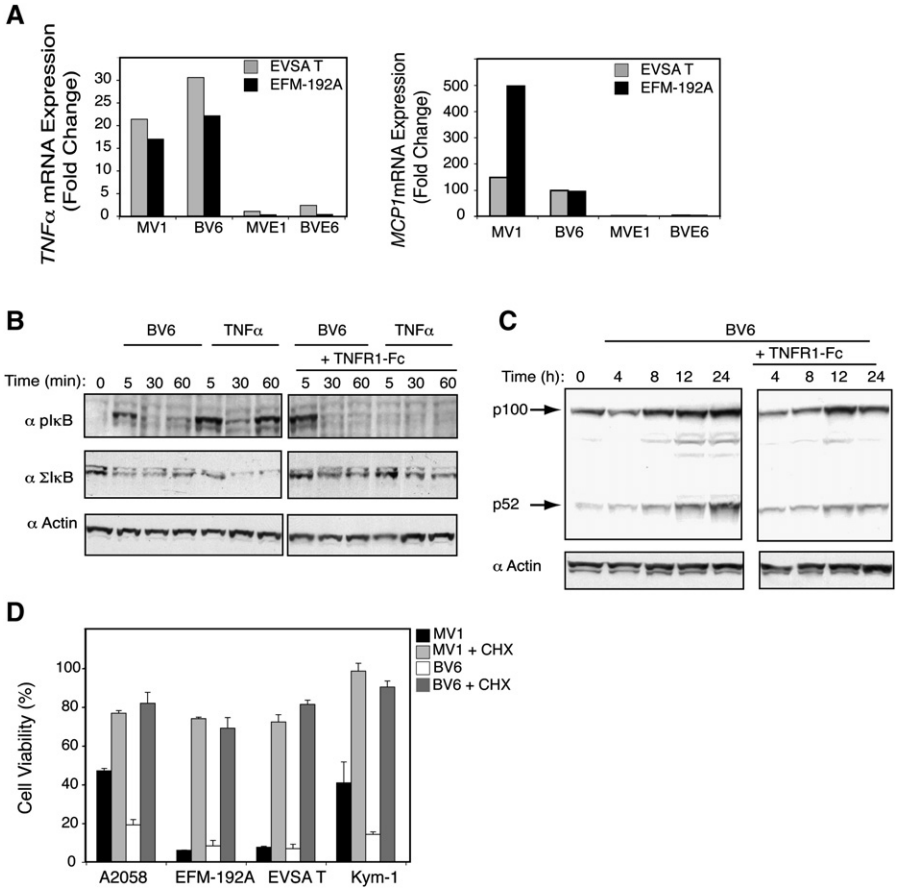

Figure 5. IAP Antagonists Activate the Canonical and Noncanonical NF-κB Pathways

(A) MV1 and BV6 stimulate *TNFα* and *MCP-1* mRNA expression. Quantitative real-time PCR analysis of *TNFα* and *MCP-1* mRNA expression was done on RNA samples derived from cells treated with MV1, BV6, MVE1, or BVE6 (5 μM) for 5 hr. All values were normalized to an *RPL19* RNA internal control.

(B) Activation of canonical NF-κB by BV6 is not inhibited by TNFR1-Fc. EFM-192A cells were treated for the indicated periods of time with TNFα (20 ng/ml) or BV6 (5 μM) in the absence or presence of TNFR1-Fc (2 μg/ml). The levels of total and phosphorylated forms of IκB were analyzed by Western blot.

(C) IAP antagonist-induced noncanonical NF-κB signaling is not inhibited by TNFR1-Fc. EVSA T cells were treated for the indicated periods of time with BV6 (5 μM) in the absence or presence of TNFR1-Fc (2 μg/ml). p100/p52 protein levels were analyzed by Western blot.

(D) Inhibition of protein expression protects cells from IAP antagonist induced cell death. Prior to administration of MV1 or BV6 (1 μM each) cells were treated with 2 μg/ml of cyclohexamide (CHX) or PBS for 2 hr. Results indicate mean with standard deviation from at least three independent experiments.

S14). However, while administration of TNFR1-Fc completely blocked TNFα activity, it did not affect BV6-stimulated phosphorylation and degradation of IκB (Figures 5B and S14). To investigate the effect of IAP antagonism on noncanonical NF-κB signaling, the effect of BV6 on the signature phosphorylation-dependent proteasomal processing of the inactive precursor NF-κB2/p100 to its active p52 form, was examined (Chen, 2005; Scheidereit, 2006). Treatment of various cell lines with BV6 resulted in the processing of precursor protein p100 to its active p52 form (Figures 5C and S15); as with IκB phosphorylation, TNFR1-Fc was unable to inhibit this activity (Figures 5C and S15). Activation of the NF-κB pathways leads to the induction of many genes, including TNFα, suggesting that de novo protein synthesis may be required for the pro-apoptotic activity of IAP antagonists. Indeed, the protein synthesis inhibitor cycloheximide (CHX) was found to significantly protect cells from IAP antagonist-induced apoptotic death (Figure 5D). Collectively, IAP antagonism induces activation of both the canonical and noncanonical NF-κB pathways, irrespective of the presence of a TNF-blocking reagent. Subsequent IAP antagonist-induced cell death requires protein synthesis, TNF signaling, and caspase activation.

c-IAP1 and c-IAP2 Promote Proteasomal Degradation of NIK

NF-κB-inducing kinase (NIK), a highly labile ser/thr kinase, is a critical regulator of the noncanonical NF-κB pathway that phosphorylates IKKα, leading to phosphorylation of

p100 and subsequent processing to p52 (Senftleben et al., 2001; Xiao et al., 2001). TRAF2, a TNFR family-binding adaptor protein negatively regulates the noncanonical NF-κB pathway, presumably by controlling the stability of NIK (Grech et al., 2004). In addition, TRAF2 exists in a preassembled complex with c-IAP1 and 2 in cells (Rothe et al., 1995; Shu et al., 1996), suggesting that c-IAP1 and 2 could be the elusive degradative E3 ligases responsible for the lability of NIK. Under this assumption IAP antagonist-induced proteasomal degradation of c-IAP1 and 2 would eliminate the candidate E3 ligases responsible for proteasomal degradation of NIK, thus allowing NIK to accumulate and trigger the noncanonical NF-κB pathway. To test this hypothesis Myc-tagged NIK was expressed in 293T cells alone or together with c-IAP1 or 2. Coexpression of NIK with c-IAP1 or 2 led to a complete loss of NIK protein (Figure 6A). However, coexpression of the RING domain mutant of c-IAP1 did not affect NIK protein levels, suggesting that ubiquitin E3 ligase activity is necessary for c-IAP1-induced degradation of NIK (Figure 6A). A c-IAP1 mutant construct that lacks the ability to associate with TRAF2 (Varfolomeev et al., 2006) was also tested and found to not affect NIK protein levels (Figure 6A). Consistent with this finding, the same c-IAP1 mutant did not associate with NIK (Figure 6B). These results suggest that TRAF2 is providing a critical scaffolding link between the ubiquitin E3 ligase c-IAP1 and its substrate NIK. Furthermore, coexpression of NIK with XIAP had no effect on NIK protein levels, demonstrating that negative regulation of NIK is not a general function of IAP proteins, but rather is limited to the TRAF2-interacting IAP proteins c-IAP1 and 2 (Figure 6A). Coexpression of c-IAP1 and NIK in the presence of proteasome inhibitor MG132 also promoted ubiquitination of NIK (Figure 6C).

Having established that c-IAP1 and 2 are ubiquitin E3 ligases capable of promoting ubiquitin-mediated proteasomal degradation of NIK, we next explored the effect of IAP antagonism on NIK stability. A 293T cell line was generated that stably expressed such low levels of labile NIK that it was only detectable following treatment with the proteasome inhibitor MG132 (Figure 6D). Treatment of this NIK-expressing cell line with the IAP antagonist BV6 triggered the expected degradation of endogenous c-IAP1 protein and led to a remarkable increase in the levels of NIK that initiated p100 processing (Figure 6D). At the same time, protein levels of TRAF2 and TRAF3 remained unchanged (Figure 6D). IAP antagonist treatment also led to stabilization of endogenous NIK as well (Figures 6E and S16). These results support a pivotal role for c-IAP1 in the degradative regulation of NIK and the noncanonical NF-κB pathway (Figure 6D). To investigate whether physiological pathways that lead to p100 processing also stimulate c-IAP1 degradation we treated several cell lines with the TNF family cytokine TWEAK (Figures 6E, 6F, and S17). Exposure to TWEAK triggered c-IAP1 degradation that was accompanied by p100 processing suggesting that c-IAPs are an inherent component of cytokine-mediated NF-κB2 activation (Figures 6F and S17). NIK protein levels increased following BV6 or TWEAK treatment and this increase was preceded by degradation of c-IAP1 consistent with the proposed role of c-IAPs as critical regulators of NIK stability (Figure 6F). Consistent with findings in human cell lines, treatment of mouse embryonic fibroblasts (MEFs) with BV6 caused rapid degradation of c-IAP1 (Figure 6G). Additionally, the processing of p100 observed in MEFs following treatment with BV6 was completely absent in NIK knock-out MEFs, demonstrating that NIK is indeed critical to mediating IAP antagonist-induced activation of the noncanonical NF-κB pathway (Figure 6G). In sum, these results suggest that c-IAPs are the E3 ligases responsible for induction of proteasomal degradation of NIK, and are thus critical regulators of the noncanonical NF-κB pathway.

DISCUSSION

Current efforts to translate fundamental understanding of cell death pathways into treatments for the eradication of cancer cells have yielded several candidate approaches that are undergoing evaluation. The ability of IAP proteins to act as inhibitors of apoptosis together with their prominent expression in human malignancies makes them attractive targets for therapeutic intervention (Hunter et al., 2007). Equally important, the feasibility of targeting IAPs to disrupt their interactions with pro-apoptotic proteins has been demonstrated (Reed, 2003). However, the mechanism by which IAP-targeting compounds initiate apoptotic signaling was not clear. In the present study we have identified critical mechanistic aspects of IAP antagonism that are important for the understanding of IAP function and their relevance in tumor biology.

Investigation of the binding of small-molecule IAP antagonists to XIAP and c-IAP1 revealed distinct differences in their interactions with the BIR domains of these proteins. While the bivalent IAP antagonist BV6 induced dimerization of c-IAP1 BIR2-BIR3, the XIAP BIR2-BIR3 protein construct remained monomeric. The observed differences are most likely the result of differential affinities of the small molecule for the BIR2 domains of c-IAP1 and XIAP (Table 1). The ability of BV6 to simultaneously engage both BIR2 and BIR3 domains of XIAP enables a more potent abrogation of XIAP-mediated caspase inhibition and potentially contributes to the higher cellular potency observed for bivalent IAP antagonists ([Gao et al., 2007] and data not shown). We have also demonstrated that both monovalent and bivalent IAP antagonists induce remarkably rapid and dramatic auto-ubiquitination and proteasomal degradation of c-IAP proteins. Although the bivalent compound is more potent, the observed activities of the monovalent and bivalent IAP antagonists are identical. This proteasomal degradation-promoting activity relies on the binding of the IAP antagonists to the BIR domains and involves RING domain-mediated auto-ubiquitination of c-IAP1 and c-IAP2 with no requirement for additional cellular factors beyond the necessary ubiquitin, and E1 and E2 enzymes. The molecular mechanism for

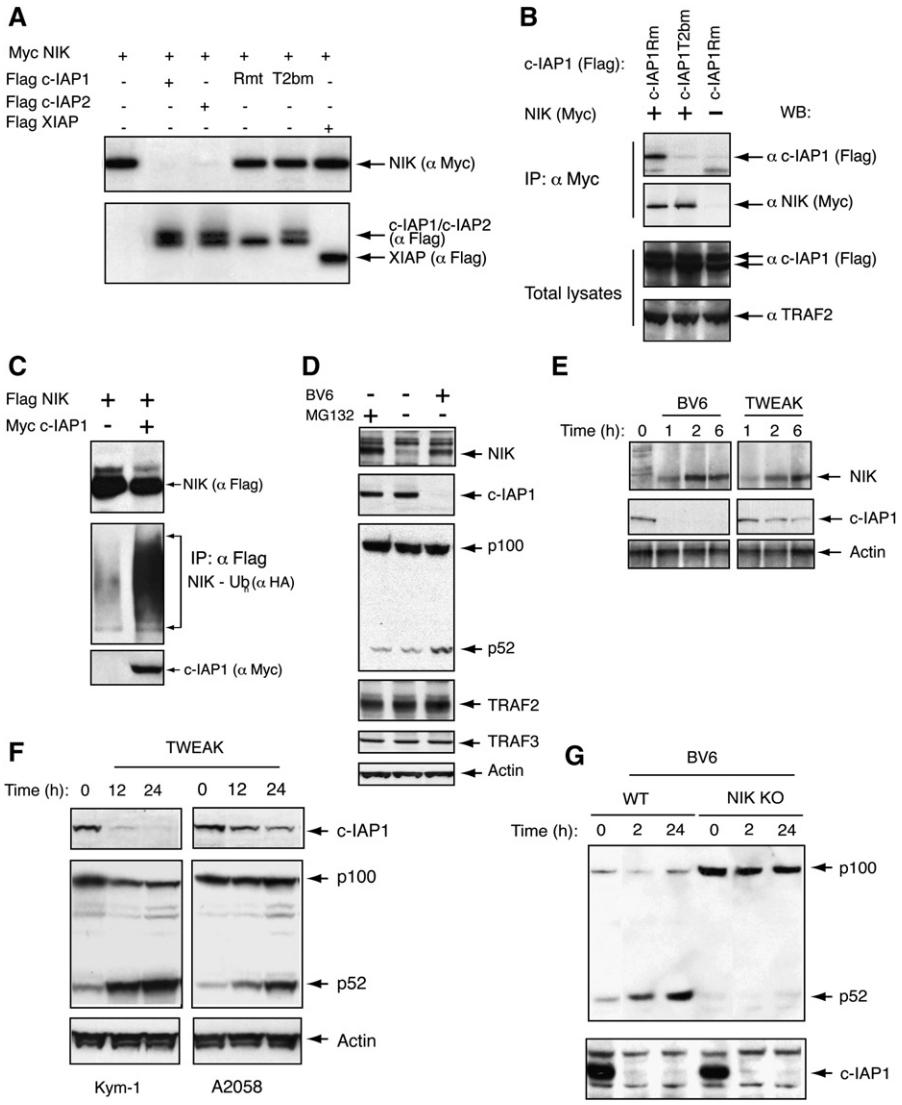

Figure 6. c-IAP1 and c-IAP2 Destabilize NIK

(A) 293T cells were transiently cotransfected with Myc-tagged NIK plasmid and indicated Flag-tagged IAP constructs. After 24 hr, cells were lysed and protein levels of ectopically expressed proteins were analyzed by Western blot analysis.

(B) c-IAP1 association with NIK requires TRAF2. 293T cells were transiently cotransfected with Myc-tagged NIK plasmid and indicated Flag-tagged c-IAP1 constructs. After 24 hr, cells were lysed and protein levels and associations were analyzed by immunoprecipitations and Western blot analysis.

(C) c-IAP1 promotes ubiquitination of NIK in cells. Flag-NIK was coexpressed in 293T cells with HA-ubiquitin and vector or Myc c-IAP1 in the presence of MG132 (20 μM). NIK expression and ubiquitination were assessed with anti-Flag and anti-HA antibodies.

(D) IAP antagonism stabilizes NIK. 293T cells stably expressing Myc-tagged NIK were treated with MG132 (20 μM) or BV6 (5 μM) for 4 hr. Proteins levels were analyzed by Western blot and indicated antibodies.

(E) IAP antagonists or TWEAK treatments lead to c-IAP1 degradation and subsequent NIK stabilization. A2058 cells were treated with BV6 (2 μM) or TWEAK (25 ng/ml) for the indicated time periods and NIK and c-IAP1 protein levels in cellular lysates were determined as described in Experimental Procedures.

(F) TWEAK triggers c-IAP1 degradation and processing of p100. Kym1 and A2058 cells were treated with TWEAK (25 ng/ml) for indicated time periods and p100/p52 and c-IAP1 protein levels in cellular lysates were determined by immunoblotting with the indicated antibodies.

(G) IAP antagonist BV6-stimulated p100 processing depends on NIK. NIK knock-out and matched wild-type mouse embryonic fibroblasts (MEFs) were treated for indicated times with BV6 (5 μM) or PBS. Following treatment cells were lysed in Nonidet P-40 lysis buffer and p100/p52 and c-IAP1 protein levels were determined by immunoblotting with indicated antibodies.

this induction of auto-ubiquitination is not entirely clear, although we speculate that the IAP antagonists disrupt an intramolecular interaction, or otherwise induce a conformational change in the c-IAP proteins that allows the ubiquitination reaction to occur. In agreement with previously published studies (Yang and Du, 2004), XIAP

appears to be spared from the IAP antagonist-stimulated auto-ubiquitination and proteasomal degradation. These findings underscore the necessity for evaluation of multiple members of the IAP family when designing antagonists with broad-spectrum affinities.

An unexpected finding was that cell death induced by IAP antagonists depends upon de novo protein biosynthesis and TNFα signaling. Given that c-IAP1 and 2 are recruited to the proximal TNFR1-signaling complexes where they cooperate with TRAF2 to suppress caspase-8 activation (Micheau and Tschopp, 2003; Wang et al., 1998), their proteasomal degradation via IAP antagonist-induced ubiquitination likely alters signaling to favor an apoptotic outcome. By negating the activity of three antiapoptotic proteins, c-IAP1 and c-IAP2 through induced auto-ubiquitination and degradation and XIAP through antagonism of caspase binding (Gao et al., 2007; Li et al., 2004; Sharma et al., 2006), IAP antagonists establish an intracellular milieu that allows caspase activation and thus advances an apoptotic fate when TNF is produced in response to IAP antagonist-induced NF-κB activation (Figure S18).

Another important discovery was the critical role of c-IAPs in the regulation of NF-κB signaling. By stimulating ubiquitin ligase activity and subsequent proteasomal degradation of c-IAP1 and c-IAP2, IAP antagonists trigger activation of the canonical and noncanonical NF-κB pathways. Noncanonical NF-κB signaling is largely controlled by NIK, a highly labile ser/thr kinase that phosphorylates IKKα; our studies identify c-IAP1 and c-IAP2 as the ubiquitin ligases responsible for its proteasomal degradation. Thus, IAP antagonists, through downregulation of c-IAPs, promote NIK stabilization and consequent activation of noncanonical NF-κB signaling (Figure S18). In addition, we have demonstrated that cytokine-mediated physiological pathways that trigger the processing of NF-κB2 (p100) involve the degradation of c-IAP1. These findings establish c-IAPs as seminal mediators of signaling pathways that activate NF-κB and provide a mechanistic insight for the recent observations that a significant proportion of multiple myeloma patients with inactivating biallelic mutations in both c-IAP1/2 have constitutive activation of the noncanonical NF-κB pathway (Annunziata et al., 2007; Keats et al., 2007).

In summary, our study provides a mechanistic explanation for the observed ability of IAP antagonists to stimulate apoptosis in cancer cells and defines novel biological roles for c-IAP1 and c-IAP2 in regulation of cellular signaling.

EXPERIMENTAL PROCEDURES

Cell Lines, Reagents, and Transfections

Hek 293T human embryonic kidney cells, A2058 human melanoma cells, HT1080 human fibrosarcoma cells, HT29 human colorectal adenocarcinoma cells, and MDA-MB-231 human breast carcinoma cells were obtained from ATCC. EVSA-T and EFM-192A human breast carcinoma cells were obtained from DSMZ. Human rhabdomyosarcoma Kym-1 cell line was obtained from HSRRB. NIK-deficient and matched wild-type mouse embryonic fibroblasts were kindly provided by Dr. Andrew Chan. HEK293T cells stably expressing NIK were established by transfection with myc-tagged NIK expression vector and hygromycin selection. Transient transfection of HEK293T cells was done using Geneporter 2 reagent (Genlantis). A2058 cells were transfected with siRNA oligonucleotides as described previously (Varfolomeev et al., 2005). All cell lines were grown in 50:50 Dulbecco's modified Eagle's and FK12 medium supplemented with 10% FBS, penicillin and streptomycin. Flag-tagged FasL was prepared as described (Sharp et al., 2005). Human recombinant soluble TNFα and TWEAK were from Genentech, Inc. Agonistic α-DR5 antibodies were purchased from R&D Systems, MN. The primary antibodies against c-IAP1 were purchased from R&D (affinity-purified goat antibody) or described previously (Varfolomeev et al., 2006; Zender et al., 2006), and we thank Dr. John Silke for his kind gift. Anti-c-IAP2 antibodies were purchased from Abcam; anti-caspase-3, -caspase-8, -XIAP, -phospho-specific IκB antibodies were from Cell Signaling Technology, Inc.; anti-caspase-9 antibody was from BD PharMingen; anti- IκB antibodies were from Cell Signaling Technology and Upstate; anti-TRAF2 and -TRAF3 antibodies were from Santa Cruz Biotechnology, Inc.; anti-Flag M2 antibody was from Sigma, anti-Myc antibody was from Roche; anti-p100/p52 antibody was from Upstate Biotechnology, anti-TRAF5 antibody was from IMGENEX; anti-Actin antibody was from ICN Biomedicals, MG132 was purchased from Calbiochem, and z-VAD-Fmk was purchased from BioMol.

Viability Assays

Cells (1–1.5 × 10^4 per well) were seeded into 96-well dishes. 8-12 hr later the media were changed, and cells were treated as indicated in the figure legends. Cell viability was measured by neutral red uptake as described (Johnston et al., 1981; Zobel et al., 2006). Long-term survival (clonogenic) assays were performed as described with 200 cells plated on 6-well plates in triplicates after indicated treatments (Franken et al., 2006).

Ubiquitination Assays

Ubiquitination assays were performed as described previously (Wertz et al., 2004). Briefly, for cell-based ubiquitination assays, 293T cells were transiently transfected as indicated and pre-treated with 20 μM MG132. 10 mM N-ethylmaleimide and 20 μM MG132 were added to the lysis buffer. Lysates were cleared by centrifugation and proteins were dissociated by heating at 95°C for 10 min. Samples were diluted, immunoprecipitated with anti-Flag antibody, and immunoblotted as indicated. Reconstituted auto-ubiquitination assays were performed in a 100 μl reaction volume with 2 μg N-terminal biotinylated ubiquitin, 0.2 μg E1, 1 μg E2 (UbcH5a) (all Boston Biochem), 0.2 μM recombinant c-IAP1 with or without 1 μM BV6 or MV1 in a buffer containing 30 mM HEPES, 2 mM DTT, and 5 mM $MgCl_2$-ATP. Reactions were incubated at 21°C for indicated time periods, stopped by adding 4 × SDS loading buffer, boiled at 95°C for 10 min, and immunoblotted with anti-c-IAP1 antibody.

Western Blot Analyses and Immunoprecipitation

Western blot analyses were performed as described previously (Varfolomeev et al., 2006; Vucic et al., 2000) using the following lysis buffer: 1% NP40, 120 mM NaCl, 50 mM HEPES, (pH 7.2), 1 mM EDTA, 10% glycerol, protease inhibitory cocktail (Roche) and MG132 (20 μM). In the case of direct lysis (Figure S3) upon treatment, cells were lysed in a buffer containing 1% SDS. Immunoprecipitation were performed as described previously (Vucic et al., 2002, 2005), the only difference being the presence of MG132 (20 μM) in the media prior to cell lysis (3 hr) and in the lysis buffer in NIK association studies. For detection of endogenous NIK protein cellular lysates were immunoprecipitated with the cocktail of anti-NIK antibodies (purchased from Chemicon, Cell Signaling, and two antibodies from Santa Cruz Biotechnology, Inc.) followed by Western blotting by anti-NIK antibody from Novus.

Analyses of Canonical and Noncanonical NF-κB Pathways

Cells were seeded into 10-cm dishes. Twelve hours before treatment, cells were washed once with PBS, and the growth media were replaced by media containing 2% heat-inactivated FBS. Cells were treated as described in the figure legends with 5 μM of IAP antagonist, or 20 ng/ml of TNFα, or 25 ng/ml of TWEAK. Cells (A2058, EVSA-T, Kym1 and EFM-192A) used in the experiments assessing p100/52 levels were treated in the presence of 20 μM of z-Vad. Following treatment cells were lysed with a kinase lysis buffer (20 mM TRIS-HCl, (pH 7.5), 150 mM NaCl, 1 mM EDTA, 1% triton, 1 × phosphatase inhibitor cocktail II [#P-5726, Sigma]) and analyzed by SDS-PAGE followed by immunoblot analysis, using anti-phospho-specific IκB or anti-total IκB antibodies, p100/p52 antibodies and ECL kit (Amersham, NY).

Supplemental Data

Supplemental Data include Supplemental Experimental Procedures, Supplemental References, eighteen figures, and three tables and can be found with this article online at http://www.cell.com/cgi/content/full/131/4/669/DC1/.

ACKNOWLEDGMENTS

We thank Ingrid Wertz, Fred Cohen, Chudi Ndubaku, Jean-Philippe Stephan, Elisabeth Blackwood, Kristina West, Mallika Singh, Stephen Gould, Karen O'Rourke, Dylan Daniel, Scot Marsters, Avi Ashkenazi, Ye Shen, Jun Liu, John Silke, David Wallach, Parameswaran Ramakrishnan, Laszlo Komuves, David Wood, members of Protein Engineering and Diagnostics departments, and the Oligo Synthesis and Sequencing facilities at Genentech that provided help with insightful discussions, suggestions, and reagents. All authors are employees and shareholders of Genentech, Inc.

Received: July 23, 2007
Revised: September 25, 2007
Accepted: October 18, 2007
Published: November 15, 2007

REFERENCES

Annunziata, C.M., Davis, R.E., Demchenko, Y., Bellamy, W., Gabrea, A., Zhan, F., Lenz, G., Hanamura, I., Wright, G., Xiao, W., et al. (2007). Frequent engagement of the classical and alternative NF-kappaB pathways by diverse genetic abnormalities in multiple myeloma. Cancer Cell *12*, 115–130.

Ashkenazi, A., and Dixit, V.M. (1999). Apoptosis control by death and decoy receptors. Curr. Opin. Cell Biol. *11*, 255–260.

Budihardjo, I., Oliver, H., Lutter, M., Luo, X., and Wang, X. (1999). Biochemical pathways of caspase activation during apoptosis. Annu. Rev. Cell Dev. Biol. *15*, 269–290.

Chen, G., and Goeddel, D.V. (2002). TNF-R1 signaling: a beautiful pathway. Science *296*, 1634–1635.

Chen, Z.J. (2005). Ubiquitin signalling in the NF-kappaB pathway. Nat. Cell Biol. *7*, 758–765.

Du, C., Fang, M., Li, Y., Li, L., and Wang, X. (2000). Smac, a mitochondrial protein that promotes cytochrome c-dependent caspase activation by eliminating IAP inhibition. Cell *102*, 33–42.

Franken, N.A., Rodermond, H.M., Stap, J., Haveman, J., and van Bree, C. (2006). Clonogenic assay of cells in vitro. Nat Protoc *1*, 2315–2319.

Gao, Z., Tian, Y., Wang, J., Yin, Q., Wu, H., Li, Y.M., and Jiang, X. (2007). A dimeric Smac/diablo peptide directly relieves caspase-3 inhibition by XIAP: Dynamic and cooperative regulation of XIAP by Smac/diablo. J. Biol. Chem., in press.

Grech, A.P., Amesbury, M., Chan, T., Gardam, S., Basten, A., and Brink, R. (2004). TRAF2 differentially regulates the canonical and noncanonical pathways of NF-κB activation in mature B cells. Immunity *21*, 629–642.

Hayden, M.S., and Ghosh, S. (2004). Signaling to NF-kappaB. Genes Dev. *18*, 2195–2224.

Hofmann, K., Bucher, P., and Tschopp, J. (1997). The CARD domain: a new apoptotic signalling motif. Trends Biochem. Sci. *22*, 155–156.

Hunter, A.M., Lacasse, E.C., and Korneluk, R.G. (2007). The inhibitors of apoptosis (IAPs) as cancer targets. Apoptosis *12*, 1543–1568.

Johnston, M.D., Finter, N.B., and Young, P.A. (1981). Dye uptake method for assay of interferon activity. Methods Enzymol. *78*, 394–399.

Kaufmann, S.H., and Vaux, D.L. (2003). Alterations in the apoptotic machinery and their potential role in anticancer drug resistance. Oncogene *22*, 7414–7430.

Keats, J.J., Fonseca, R., Chesi, M., Schop, R., Baker, A., Chng, W.J., Van Wier, S., Tiedemann, R., Shi, C.X., Sebag, M., et al. (2007). Promiscuous mutations activate the noncanonical NF-kappaB pathway in multiple myeloma. Cancer Cell *12*, 131–144.

Li, L., Thomas, R.M., Suzuki, H., De Brabander, J.K., Wang, X., and Harran, P.G. (2004). A small molecule Smac mimic potentiates TRAIL- and TNFα-mediated cell death. Science *305*, 1471–1474.

Li, X., Yang, Y., and Ashwell, J.D. (2002). TNF-RII and c-IAP1 mediate ubiquitination and degradation of TRAF2. Nature *416*, 345–347.

Liston, P., Fong, W.G., and Korneluk, R.G. (2003). The inhibitors of apoptosis: there is more to life than Bcl2. Oncogene *22*, 8568–8580.

Liu, Z., Sun, C., Olejniczak, E.T., Meadows, R.P., Betz, S.F., Oost, T., Herrmann, J., Wu, J.C., and Fesik, S.W. (2000). Structural basis for binding of Smac/DIABLO to the XIAP BIR3 domain. Nature *408*, 1004–1008.

Micheau, O., and Tschopp, J. (2003). Induction of TNF receptor I-mediated apoptosis via two sequential signaling complexes. Cell *114*, 181–190.

Miller, L.K. (1999). An exegesis of IAPs: salvation and surprises from BIR motifs. Trends Cell Biol. *9*, 323–328.

Oost, T.K., Sun, C., Armstrong, R.C., Al-Assaad, A.S., Betz, S.F., Deckwerth, T.L., Ding, H., Elmore, S.W., Meadows, R.P., Olejniczak, E.T., et al. (2004). Discovery of potent antagonists of the antiapoptotic protein XIAP for the treatment of cancer. J. Med. Chem. *47*, 4417–4426.

Reed, J.C. (2003). Apoptosis-targeted therapies for cancer. Cancer Cell *3*, 17–22.

Rothe, M., Pan, M.G., Henzel, W.J., Ayres, T.M., and Goeddel, D.V. (1995). The TNFR2-TRAF signaling complex contains two novel proteins related to baculoviral inhibitor of apoptosis proteins. Cell *83*, 1243–1252.

Rothe, M., Wong, S.C., Henzel, W.J., and Goeddel, D.V. (1994). A novel family of putative signal transducers associated with the cytoplasmic domain of the 75 kDa tumor necrosis factor receptor. Cell *78*, 681–692.

Salvesen, G.S., and Abrams, J.M. (2004). Caspase activation - stepping on the gas or releasing the brakes? Lessons from humans and flies. Oncogene *23*, 2774–2784.

Salvesen, G.S., and Duckett, C.S. (2002). IAP proteins: blocking the road to death's door. Nat. Rev. Mol. Cell Biol. *3*, 401–410.

Samuel, T., Welsh, K., Lober, T., Togo, S.H., Zapata, J.M., and Reed, J.C. (2006). Distinct BIR domains of cIAP1 mediate binding to and ubiquitination of tumor necrosis factor receptor-associated factor 2 and second mitochondrial activator of caspases. J. Biol. Chem. *281*, 1080–1090.

Scheidereit, C. (2006). IκB kinase complexes: gateways to NF-κB activation and transcription. Oncogene *25*, 6685–6705.

Senftleben, U., Cao, Y., Xiao, G., Greten, F.R., Krahn, G., Bonizzi, G., Chen, Y., Hu, Y., Fong, A., Sun, S.C., and Karin, M. (2001). Activation by IKKα of a second, evolutionary conserved, NF-κB signaling pathway. Science *293*, 1495–1499.

Sharma, S.K., Straub, C., and Zawel, L. (2006). Development of peptidomimetics targeting IAPs. International Journal of Peptide Research and Therapeutics *12*, 21–32.

Sharp, D.A., Lawrence, D.A., and Ashkenazi, A. (2005). Selective knockdown of the long variant of cellular FLICE inhibitory protein augments death receptor-mediated caspase-8 activation and apoptosis. J. Biol. Chem. *280*, 19401–19409.

Shu, H.B., Takeuchi, M., and Goeddel, D.V. (1996). The tumor necrosis factor receptor 2 signal transducers TRAF2 and c-IAP1 are components of the tumor necrosis factor receptor 1 signaling complex. Proc. Natl. Acad. Sci. USA *93*, 13973–13978.

Steller, H. (1995). Mechanisms and genes of cellular suicide. Science *267*, 1445–1449.

Sun, H., Nikolovska-Coleska, Z., Yang, C.Y., Xu, L., Liu, M., Tomita, Y., Pan, H., Yoshioka, Y., Krajewski, K., Roller, P.P., and Wang, S. (2004). Structure-based design of potent, conformationally constrained Smac mimetics. J. Am. Chem. Soc. *126*, 16686–16687.

Thompson, C.B. (1995). Apoptosis in the pathogenesis and treatment of disease. Science *267*, 1456–1462.

Varfolomeev, E., Maecker, H., Sharp, D., Lawrence, D., Renz, M., Vucic, D., and Ashkenazi, A. (2005). Molecular determinants of kinase pathway activation by Apo2 ligand/tumor necrosis factor-related apoptosis-inducing ligand. J. Biol. Chem. *280*, 40599–40608.

Varfolomeev, E., Wayson, S.M., Dixit, V.M., Fairbrother, W.J., and Vucic, D. (2006). The inhibitor of apoptosis protein fusion c-IAP2.MALT1 stimulates NF-κB activation independently of TRAF1 AND TRAF2. J. Biol. Chem. *281*, 29022–29029.

Vaux, D.L., and Silke, J. (2005). IAPs, RINGs and ubiquitylation. Nat. Rev. Mol. Cell Biol. *6*, 287–297.

Verhagen, A.M., Ekert, P.G., Pakusch, M., Silke, J., Connolly, L.M., Reid, G.E., Moritz, R.L., Simpson, R.J., and Vaux, D.L. (2000). Identification of DIABLO, a mammalian protein that promotes apoptosis by binding to and antagonizing IAP proteins. Cell *102*, 43–53.

Vucic, D., Deshayes, K., Ackerly, H., Pisabarro, M.T., Kadkhodayan, S., Fairbrother, W.J., and Dixit, V.M. (2002). SMAC Negatively Regulates the Anti-apoptotic Activity of Melanoma Inhibitor of Apoptosis (ML-IAP). J. Biol. Chem. *277*, 12275–12279.

Vucic, D., Franklin, M.C., Wallweber, H.J., Das, K., Eckelman, B.P., Shin, H., Elliott, L.O., Kadkhodayan, S., Deshayes, K., Salvesen, G.S., and Fairbrother, W.J. (2005). Engineering ML-IAP to produce an extraordinarily potent caspase 9 inhibitor: implications for Smac-dependent anti-apoptotic activity of ML-IAP. Biochem. J. *385*, 11–20.

Vucic, D., Stennicke, H.R., Pisabarro, M.T., Salvesen, G.S., and Dixit, V.M. (2000). ML-IAP, a novel inhibitor of apoptosis that is preferentially expressed in human melanomas. Curr. Biol. *10*, 1359–1366.

Wang, C.Y., Mayo, M.W., Korneluk, R.G., Goeddel, D.V., and Baldwin, A.S., Jr. (1998). NF-κB antiapoptosis: induction of TRAF1 and TRAF2 and c-IAP1 and c-IAP2 to suppress caspase-8 activation. Science *281*, 1680–1683.

Wertz, I.E., O'Rourke, K.M., Zhou, H., Eby, M., Aravind, L., Seshagiri, S., Wu, P., Wiesmann, C., Baker, R., Boone, D.L., et al. (2004). De-ubiquitination and ubiquitin ligase domains of A20 downregulate NF-κB signalling. Nature *430*, 694–699.

Wu, G., Chai, J., Suber, T.L., Wu, J.W., Du, C., Wang, X., and Shi, Y. (2000). Structural basis of IAP recognition by Smac/DIABLO. Nature *408*, 1008–1012.

Xiao, G., Harhaj, E.W., and Sun, S.C. (2001). NF-κB-inducing kinase regulates the processing of NF-κB2 p100. Mol. Cell *7*, 401–409.

Yang, Q.H., and Du, C. (2004). Smac/DIABLO selectively reduces the levels of c-IAP1 and c-IAP2 but not that of XIAP and livin in HeLa cells. J. Biol. Chem. *279*, 16963–16970.

Yang, Y., Fang, S., Jensen, J.P., Weissman, A.M., and Ashwell, J.D. (2000). Ubiquitin protein ligase activity of IAPs and their degradation in proteasomes in response to apoptotic stimuli. Science *288*, 874–877.

Zender, L., Spector, M.S., Xue, W., Flemming, P., Cordon-Cardo, C., Silke, J., Fan, S.T., Luk, J.M., Wigler, M., Hannon, G.J., et al. (2006). Identification and validation of oncogenes in liver cancer using an integrative oncogenomic approach. Cell *125*, 1253–1267.

Zobel, K., Wang, L., Varfolomeev, E., Franklin, M.C., Elliott, L.O., Wallweber, H.J., Okawa, D.C., Flygare, J.A., Vucic, D., Fairbrother, W.J., and Deshayes, K. (2006). Design, synthesis, and biological activity of a potent Smac mimetic that sensitizes cancer cells to apoptosis by antagonizing IAPs. ACS Chem Biol *1*, 525–533.